

Generation of Singlet Molecular Oxygen from H₂O₂ with Molybdate-Exchanged Layered Double Hydroxides: Effects of Catalyst Composition and Reaction Conditions

F. M. P. R. van Laar,^{*} D. E. De Vos,^{*} F. Pierard,[†] A. Kirsch-De Mesmaeker,[†]
L. Fiermans,[‡] and P. A. Jacobs^{1,*}

^{*}Centre for Surface Chemistry and Catalysis, K. U. Leuven, Kardinaal Mercierlaan 92, B-3001 Heverlee, Belgium; [†]Physical Organic Chemistry, CP160/08, Université Libre de Bruxelles, 50 Av. F.D. Roosevelt, B-1050 Brussels, Belgium; and [‡]Department of Solid State Sciences, Ghent University, Krijgslaan 281/S1, B-9000 Gent, Belgium

Received June 12, 2000; revised August 14, 2000; accepted August 28, 2000

(Mg, Al)-layered double hydroxides (LDHs) with different Mg/Al ratios in the octahedral layer were prepared via the coprecipitation method and were exchanged with varying amounts of molybdate. The composition of the LDH supports and the state of the molybdate in these materials were studied with X-ray diffractometry, X-ray photoelectron spectroscopy and Raman. As was proven by NIR luminescence, aqueous H₂O₂ is converted at the surface of these catalysts into excited, singlet molecular dioxygen (¹O₂). The singlet dioxygen diffuses away from the ¹O₂ generating centers and can perform selective oxygenations, such as endoperoxidations of dienes, or hydroperoxidations of olefins. Catalyst composition and reaction conditions (temperature, solvent) have major effects on the catalyzed ¹O₂ generation and the subsequent substrate oxygenation. In order to maximize the efficiency of the H₂O₂ use and to limit the epoxidation side reaction, it is advisable to limit the amount of exchanged molybdate to ~0.2 mmol per g and to use an LDH with Mg_{0.9}Al_{0.1} composition in the octahedral layer. The latter material provides the optimum basicity for the catalytic activity of the exchanged molybdate. © 2001 Academic Press

Key Words: molybdate; layered double hydroxides; hydrogen peroxide; singlet dioxygen; peroxidation.

INTRODUCTION

Selective oxyfunctionalization of organic compounds by singlet molecular oxygen has received much attention since the 1960s, because of the unique reactivity of ¹O₂ and its highly selective reaction with electron-rich organic substrates such as olefins. Typical ¹O₂ products include enyl hydroperoxides, dioxetanes and endoperoxides (1). Reactions of ¹O₂ thus essentially differ in regio- and chemoselectivity from those of radical or electrophilic agents such as RO[•] or ROO[•] radicals or (in)organic peracids (2).

The literature contains elaborate studies of photosensitization for the generation of singlet molecular oxygen. However, due to the rather low stability of the “old generation” dyes (such as methylene blue, rose bengal) under photooxidative conditions (3–7), there has been an intensive search for more stable sensitizers like halogenated porphyrins (8, 9) and for alternative “dark” systems. These dark systems are based on the conversion of hydrogen peroxide into water and singlet molecular oxygen (10). ¹O₂ can be generated by stoichiometric reaction of H₂O₂ with ClO⁻, but the reaction produces salt waste and the rate of this reaction is not easily controlled. Moreover, depending on the pH and on the substrate molecule, the use of the electrophilic hypochlorite may lead to undesired halogenations. Early reports from the 1970s mention that some transition metals, such as Ti^{IV} and Mo^{VI}, may catalytically generate one molecule of singlet molecular oxygen from two molecules hydrogen peroxide (11, 12). Later, screening of the periodic table revealed four groups of inorganic compounds capable of generating singlet molecular oxygen from hydrogen peroxide (13).

Several studies have been devoted to the use of homogeneous molybdate catalysts. High alkalinity, with a pH between 10 and 11, is required for a fast and efficient singlet molecular oxygen generation. The reaction proceeds efficiently only in pure water, in aqueous MeOH and EtOH. For reactions with highly apolar substrates, a reverse microemulsion may be used, in which ¹O₂ is generated in the aqueous droplets, while the oxygenation takes place in the continuous organic phase (14). However, the system has several drawbacks: if catalytic amounts of molybdate are used, soluble base is needed to adjust the pH and relatively large solvent volumes are used. Only one truly immobilized molybdate system has been reported by McGoran and Wyborney (15), with molybdate immobilization on an anion exchanging Amberlyst resin.

¹ To whom correspondence should be addressed. Fax: 32 16 32 1998. E-mail: pierre.jacobs@agr.kuleuven.ac.be.

We have recently reported on a molybdate-exchanged layered double hydroxide (LDH), which is a heterogeneous catalyst for conversion of H_2O_2 into $^1\text{O}_2$ (16). The use of such a heterogeneous catalyst allows working with catalytic amounts of molybdate without extra dissolved base, and should allow more freedom in the choice of an appropriate solvent for the substrate molecule. LDHs are simple inorganic anion exchangers, which are analogous to the mineral Hydrotalcite $[\text{Mg}_6\text{Al}_2(\text{OH})_{16}](\text{CO}_3) \cdot 4\text{H}_2\text{O}$ (17, 18). The focus of the present work is to study the behavior of these molybdate LDH catalysts as a function of their composition and of the reaction conditions. A first, physicochemical part, studies the changes of the catalyst when the Mg/Al ratio in the octahedral layer or the Mo content are varied. The catalyst is studied with *ex situ* techniques as well as under catalytic conditions. Particular attention is devoted to the characterization of the basic properties of the host material via several complementary methods (19, 20). Next, some parameters that affect the catalytic properties of the LDH catalyst are studied in test reactions. Important variables are Mo content, Mg/Al ratio in the support, hydrophilicity of the catalyst, temperature, and solvent. Relations are sought between the properties of the LDH (e.g., basicity) and reaction characteristics such as product selectivity. This optimization leads to the design of improved reaction conditions that are applied in the selective oxyfunctionalization of organic molecules such as dienes.

EXPERIMENTAL

Catalyst Preparation

Layered double hydroxides are easily synthesized by coprecipitation at low supersaturation. All syntheses and exchanges are performed, according to literature procedures at a constant pH of 10 ± 0.5 and under nitrogen atmosphere to avoid CO_2 contamination (17). In order to obtain $\text{Mg}_x\text{Al}_{(1-x)}\text{A}_{(1-x)}(\text{OH})_2 \cdot m\text{H}_2\text{O}$, with A a monovalent anion such as Cl^- or NO_3^- , equal volumes of decarbonated solutions of $\text{MgCl}_2 \cdot 6\text{H}_2\text{O}$ or $\text{Mg}(\text{NO}_3)_2 \cdot 6\text{H}_2\text{O}$ (xM , 200 ml) and $\text{AlCl}_3 \cdot 6\text{H}_2\text{O}$ or $\text{Al}(\text{NO}_3)_3 \cdot 9\text{H}_2\text{O}$ ($(1-x)M$, 200 ml) are slowly added to 80 ml H_2O . To maintain the pH at 10, addition of 1.5 M NaOH is required. The LDH is obtained after 18 h aging at room temperature, centrifuged, washed, and freeze-dried. Overnight exchange of 1.5 g LDH in 100 ml 2.8–11.2 mM solutions of $\text{Na}_2\text{MoO}_4 \cdot 2\text{H}_2\text{O}$ (pH 10, room temperature, N_2 atmosphere) yields the hydrophilic molybdate exchanged Mg, Al-LDH materials (LDH-Mo).

In a similar procedure, the organic anion *p*-toluenesulfonate (pTOS) is coexchanged with molybdate on the LDH to yield a more hydrophobic molybdate catalyst, further denoted as LDH-MopTOS. $\text{Mg}_{0.7}\text{Al}_{0.3}$ -MopTOS (MoO₄ 12.5%, pTOS 87.5% of the anion exchange capacity) is obtained by mixing 9 mmol pTOS and 0.5625 mmol $\text{Na}_2\text{MoO}_4 \cdot 2\text{H}_2\text{O}$ in 150 ml decarbonated water, correcting

the pH to 10, and adding 1.5 g of LDH. For $\text{Mg}_{0.7}\text{Al}_{0.3}$ -MopTOS (MoO₄ 25%, pTOS 75%) 4.5 mmol pTOS and 1.125 mmol $\text{Na}_2\text{MoO}_4 \cdot 2\text{H}_2\text{O}$ were used. The exchange is typically performed at pH 10, for 18 h at 65°C, subsequently for 18 h at room temperature, all under N_2 atmosphere.

Catalyst Characterization

The lattice structure of the LDHs was determined using powder X-ray diffraction with a Siemens D 5000 matic diffractometer and Ni-filtered $\text{CuK}\alpha$ radiation (8048 eV). The surface composition of the LDH samples was analyzed by X-ray photoelectron spectroscopy (XPS) with a Perkin Elmer PHI 5500 ESCA system, using monochromatic $\text{AlK}\alpha$ radiation (1486.6 eV). The integrated areas of the O 1s, Mg 2s, Al 2s, S 2s, and Mo $3d_{3/2}$ -Mo $3d_{5/2}$ lines were used to calculate the atomic ratio of the elements. The XPS binding energies were calibrated with the C 1s line at 286.4 eV as a reference. For samples containing sulfur, an overlap between the S 2s and Mo $3d_{5/2}$ lines is observed. In these cases, deconvolution was performed by calculating the S 2s area from the S 2p area. Moreover, the Mo 3p peak was used in order to check the quantification of the Mo 3d lines. Bulk elemental analyses of Mg, Al, and Mo were carried out by emission spectroscopy with inductively coupled plasma (ICP), after dissolution of the LDH samples in 14% HNO_3 . FT-Raman spectra were recorded with a Bruker IFS 100 spectrometer; samples were analyzed using a CW Nd:YAG laser at 150–450 mW. Scanning electron micrographs (SEM) were taken on a Philips XL 33.

UV-vis diffuse reflectance spectra (DRS) were recorded on a Cary 5 spectrophotometer, using anhydrous BaSO_4 as the standard over the whole spectral range. Near infrared (NIR) luminescence (IRL) spectra were recorded with a liquid N_2 cooled Ge detector of North Coast (EO 817-L) connected with a lock-in amplifier and muon filter. The Ge detector was attached to an Edinburgh fluorimeter (CD 900). Experiments to determine the basic properties of the layered double hydroxides with the use of indicators were performed as follows: 0.15 g LDH was vacuum dried at room temperature for 24 h and was mixed with 2 ml indicator solution (0.1 mg bromothymol blue, phenolphthalein or alizarin per ml dry toluene). Suspensions containing bromothymol blue and phenolphthalein were titrated with a 0.01 M solution of benzoic acid in toluene. Samples with adsorbed alizarin were filtered, vacuum dried, and analyzed with DRS.

Catalytic Reactions and Characterization of Reaction Products

Hydrogen peroxide concentrations were derived from cerimetric titrations, using a 0.1 N Ce^{IV} solution. Samples were acidified with HCl prior to titration.

Reaction mixtures were analyzed on a GC equipped with a 50-m CP-Sil 5 column. Samples were taken after complete hydrogen peroxide conversion (catalyst becomes white again). Mixtures containing enyl hydroperoxides were reduced with an excess triphenylphosphine (PPh_3) prior to GC analysis; the (exothermic) reduction is complete after a few minutes. Product identity was checked with GC-MS on a MD 800 mass spectrometer of Fisons in combination with known fragmentation patterns (21) or with the use of photosensitization. Characteristic fragment ions of some important products are endoperoxide from 1,3-cyclohexadiene, $m/z = 112, 83, 80, 68, 55$; endoperoxide from 2,3-dimethyl-1,3-butadiene, $m/z = 114, 96, 85, 82, 67$; endoperoxide from *cis,cis*-1,3-cyclooctadiene, $m/z = 140, 122, 111, 97, 79$; ascaridole (endoperoxide from α -terpinene), $m/z = 168, 136, 121, 93, 79$.

Products

Products were purchased in the highest purities available and used as obtained: bromothymol blue, hydrochloric acid, and dimethylformamide (DMF) from Merck, phenolphthalein and $\text{AlCl}_3 \cdot 6\text{H}_2\text{O}$ from UCB, alizarin, hydrogen peroxide (35% in H_2O), $\text{Ce}(\text{SO}_4)_2 \cdot 4\text{H}_2\text{O}$, $\text{Mg}(\text{NO}_3)_2 \cdot 6\text{H}_2\text{O}$, NaOH, *p*-toluenesulfonic acid, 1-methyl-1-cyclohexene, α -terpinene, 1,3-cyclohexadiene, 1,4-dioxane, and tetrahydrofuran (THF) from Acros, benzoic acid, $\text{Na}_2\text{MoO}_4 \cdot 2\text{H}_2\text{O}$, $(\text{NH}_4)_6\text{Mo}_7\text{O}_{24} \cdot 4\text{H}_2\text{O}$, 2,3-dimethyl-2-butene, 2,3-dimethyl-1,3-butadiene, *cis,cis*-1,3-cyclooctadiene, and (-)- β -citronellol from Aldrich, $\text{Al}(\text{NO}_3)_3 \cdot 9\text{H}_2\text{O}$, bengal rose, and 2-methyl-2-pentene from Fluka, toluene, acetonitrile, and acetone from Biosolve LTD, $\text{MgCl}_2 \cdot 6\text{H}_2\text{O}$ from VEL, ethanol from BDH, and methanol and 2-propanol from Riedel-de-Haën.

RESULTS AND DISCUSSION

Structural Characterization of the Layered Double Hydroxides

The nominal chemical composition, the bulk and surface composition, and the crystalline phases in the as-synthesized layered double hydroxides with varying Mg/Al ratio are shown in Table 1. For all samples, the XRD patterns clearly show an LDH crystalline phase, with Hydrotalcite structure (Fig. 1). When the aluminum content is low (10% of the octahedrally coordinated atoms; $\text{Mg}_{0.9}\text{Al}_{0.1}$ -LDH), a Brucite phase ($\text{Mg}(\text{OH})_2$) is detected, with characteristic reflections at 18.5, 38, 50.8, 58.8, and 62.2° 2θ . Further lowering the Al content of the support is not relevant, since the specific anion exchange capacity of these mixed hydrotalcite-brucite samples becomes quite small. The broad diffraction lines of the layered double hydroxides indicate the presence of rather small crystallites, which was confirmed with scanning electron micrographs. Crystallite size is estimated at 100–150 nm. The *a* lattice parameter

TABLE 1

Layered Double Hydroxide Supports: Chemical Composition and XRD Characterization

Sample, nominal composition	$x = \text{Al}/(\text{Al} + \text{Mg})$		XRD analysis phase	Lattice parameter, $a = 2d_{[110]}$ (Å)
	Bulk, ICP	Surface, XPS		
$\text{Mg}_{0.7}\text{Al}_{0.3}$ -LDH	0.32	0.32	Hydrotalcite	3.050
$\text{Mg}_{0.8}\text{Al}_{0.2}$ -LDH	0.22	0.28	Hydrotalcite	3.080
$\text{Mg}_{0.9}\text{Al}_{0.1}$ -LDH	0.13	0.17	Hydrotalcite + Brucite	3.094

of the samples decreases from its initial value for Brucite ($a = 3.146$ Å) as the Al content increases (Table 1). This contraction of the hydrotalcite unit cell can be rationalized by the isomorphous substitution of the larger Mg^{2+} cation by the smaller Al^{3+} cation (ionic radius of $\text{Mg}^{2+} = 65$ pm and of $\text{Al}^{3+} = 50$ pm) (22).

For the samples with an Al content lower than 30%, XPS detects a surface enrichment of Al. This seems in line with a gradual phase separation as the composition of the material deviates from the limiting hydrotalcite composition ($\text{Mg}_{0.75}\text{Al}_{0.25}$ -LDH). As indicated by the XRD data, brucite is formed as a separate phase; the XPS data suggest that for $\text{Mg}_{0.8}\text{Al}_{0.2}$ -LDH and $\text{Mg}_{0.9}\text{Al}_{0.1}$ -LDH an Al-rich LDH phase is formed on top of the brucite phase, resulting in an apparent surface enrichment with Al.

As shown in Fig. 1, the difference between a hydrophilic LDH-Mo and an expanded, hydrophobic LDH-MopTOS can easily be investigated with XRD. The decrease of the 2θ value of the d_{003} line corresponds to an increase of the basal spacing from 7.6 Å up to 17.25 Å for the pTOS pillared LDH. This value is in good agreement with the value

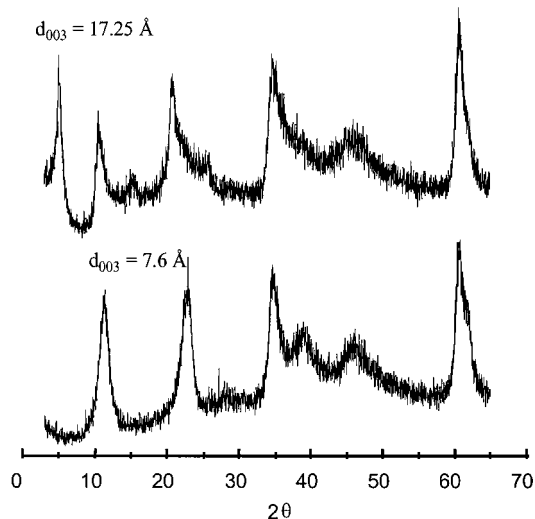


FIG. 1. XRD patterns of (bottom) hydrophilic $\text{Mg}_{0.7}\text{Al}_{0.3}$ -LDH-Mo (MoO_4^{2-} , 25% of AEC; 75% NO_3^-) and (top) $\text{Mg}_{0.7}\text{Al}_{0.3}$ -LDH-MopTOS (MoO_4^{2-} , 25% of AEC; 75% pTos).

TABLE 2
Mo and S Content of MoO_4^{2-} or MoO_4^{2-} , pTOS Exchanged Layered Double Hydroxides ($\text{Mg}_{0.7}\text{Al}_{0.3}$ -LDH) as Determined by Bulk Analysis or XPS

	Nominal composition of AEC (%)		Mo/Al ratio		S/Al ratio (XPS)
			Bulk (ICP)	Surface (XPS)	
1	12.5% MoO_4^{2-}	87.5% NO_3^-	0.064	0.053	—
2	25% MoO_4^{2-}	75% NO_3^-	0.104	0.105	—
3	37.5% MoO_4^{2-}	62.5% NO_3^-	0.143	0.138	—
4	50% MoO_4^{2-}	50% NO_3^-	0.255	0.19	—
5	12.5% MoO_4^{2-}	87.5% pTOS	—	0.07	0.86
6	25% MoO_4^{2-}	75% pTOS	—	0.104	0.79

calculated in the assumption that the anions are perpendicularly oriented between the layers (23). Such a perpendicular orientation is probable given the high surface charge of the layered double hydroxides. Moreover, the XPS data (Table 2, entries 5 and 6) indicate that apart from molybdate, only *para*-toluenesulfonate is present as a counter anion; in these LDH-MopTOS, which were prepared starting from a chloride exchanged LDH, no Cl could be detected by XPS.

Characterization of Immobilized Molybdenum

In order to properly evaluate the catalytic data, it is important to study the state of the exchanged Mo, particularly when the molybdate concentration on the catalyst is increased. Comparison of XPS and bulk elemental analysis demonstrates that molybdenum is homogeneously dispersed throughout the support (Table 2, entries 1–4); there is no evidence for accumulation of Mo as clusters on the outer surface. The XPS Mo $3d_{3/2}$ and Mo $3d_{5/2}$ lines are located at 235.50 and 232.35 eV, respectively, which is characteristic for MoO_4^{2-} (24). No other Mo lines, such as of heptamolybdate (Mo $3d_{3/2}$ and Mo $3d_{5/2}$ located at 237.2 and 234.3 eV) were observed.

As the molybdenum-oxygen vibrations in the infrared region ($800\text{--}1000\text{ cm}^{-1}$) severely overlap with the absorptions of the support, Raman spectroscopy was applied. All molybdate-exchanged layered double hydroxides show a clear vibration at 896 cm^{-1} . The latter is assigned to the Mo–O symmetrical stretching vibration of MoO_4^{2-} . Only for the sample with the highest molybdate loading ($\text{Mg}_{0.7}\text{Al}_{0.3}$ -LDH exchanged with MoO_4^{2-} , 50% of the AEC) a supplementary band is observed at 940 cm^{-1} . Based on literature, this band may be identified as the most intense band of polymerized Mo species such as heptamolybdate (25, 26). Weaker bands, e.g., the Mo–O–Mo ν and δ vibrations of $\text{Mo}_7\text{O}_{24}^{6-}$ located at 564 and 219 cm^{-1} respectively, could not clearly be discerned in the spectrum. The failure of XPS to detect other species than MoO_4^{2-} might be due to the relatively low sensitivity of the technique; on the other hand, it

cannot be excluded that the Raman observation of a minor amount of polymerized Mo is due to local overheating of the sample in the laser beam. Anyhow, in view of the very limited changes in d-spacing in the X-ray diffractograms, it is excluded that the major part of Mo is present as $\text{Mo}_7\text{O}_{24}^{6-}$, since the limited interlayer spacing does not allow stacking of these bulky $\text{Mo}_7\text{O}_{24}^{6-}$ anions between the LDH sheets.

Summarizing, both XPS and Raman convincingly prove that, even for samples with a Mo content up to 50% of the anion exchange capacity, the major part of molybdenum is present as non-polymerized MoO_4^{2-} . This is in accordance with the conditions of the molybdate ion exchanges, which were performed at a pH of 10; note that heptamolybdate is rather formed and stable in more acidic solutions (pH about 4).

Catalyst Characterization in Reaction Conditions

Time-resolved UV-vis diffuse reflectance spectroscopy (DRS) in combination with infrared luminescence (IRL) can be used to investigate respectively the formation of the $^1\text{O}_2$ precursors and of singlet molecular oxygen itself. In molybdenum-catalyzed reactions, $^1\text{O}_2$ can be released from di-, tri-, and tetraperoxomonomolybdate species (27–30). While the triperoxomolybdate $\text{MoO}(\text{O}_2)_3^{3-}$ is hard to detect with UV-vis spectroscopy, ^{95}Mo -NMR/kinetic experiments on concentrated molybdate solutions indicate that particularly this triperoxo species easily forms singlet molecular oxygen, while $^1\text{O}_2$ release is slower from di- and tetraperoxomolybdates. Exposure of the solid LDH-Mo catalyst to a hydrogen peroxide solution results in a brick-red material. DRS study of this material shows the appearance of two distinct new absorptions, one around $32,000\text{ cm}^{-1}$ (310 nm) and the other around $22,000\text{ cm}^{-1}$ (455 nm) (Fig. 2). Based on solution UV-vis data (31–33), these absorptions can be ascribed to the yellow diperoxomolybdate $\text{MoO}_2(\text{O}_2)_2^{2-}$ (310 nm) and the tetraperoxomolybdate $\text{Mo}(\text{O}_2)_4^{2-}$ (455 nm). The simultaneous presence of the di- and tetraperoxomolybdate indicates that the triperoxomolybdate must be present as an intermediate species. The

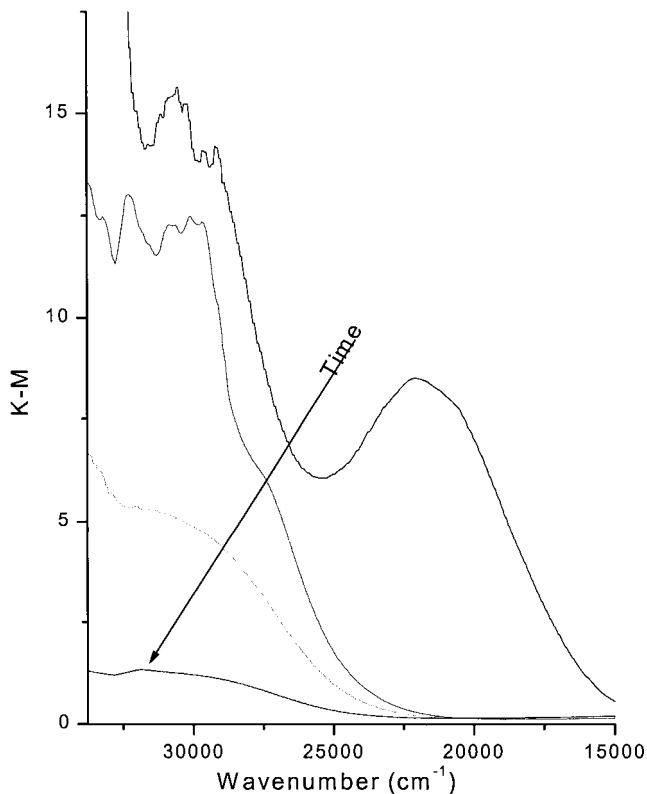
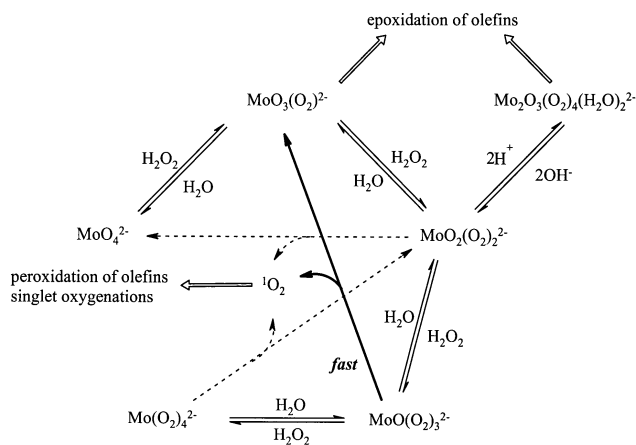


FIG. 2. Diffuse reflectance spectra as a function of time of $\text{Mg}_{0.7}\text{Al}_{0.3}$ -LDH- MoO_4 (AEC 37.5%), wetted with a dilute H_2O_2 solution in 1,4-dioxane, K-M, Kubelka-Munk.

shoulder observed around $27,500\text{ cm}^{-1}$ (365 nm) may tentatively be assigned to this triperoxo species, in agreement with the proposals of Aubry and Csányi (29, 31). Hence, the species that are known to generate $^1\text{O}_2$ in solution, are also present at the surface of the LDH-Mo catalyst. The interactions of LDH-Mo with hydrogen peroxide are summarized in Scheme 1.



SCHEME 1. Possible interactions of molybdate with H_2O_2 at the surface of an LDH.

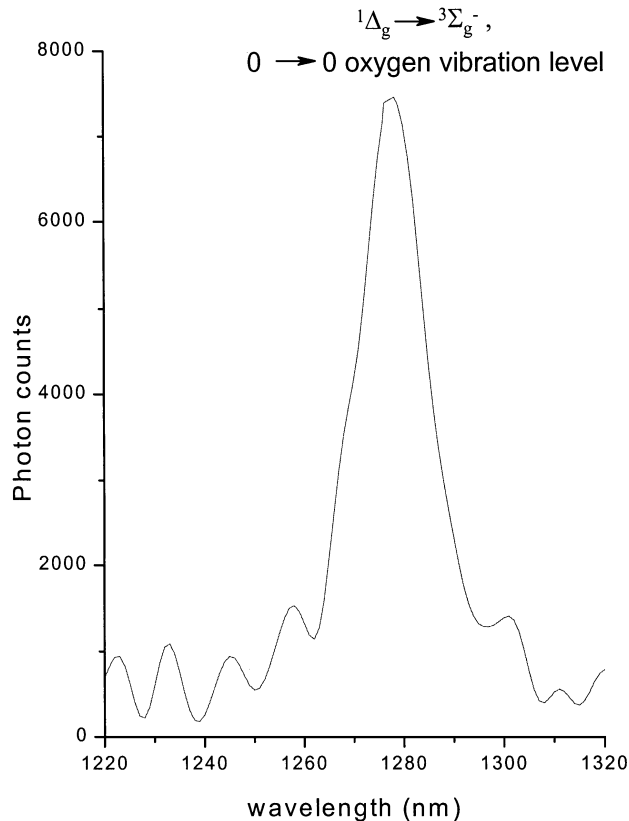


FIG. 3. Infrared luminescence of $^1\text{O}_2$ in the catalytic disproportionation of H_2O_2 by LDH- MoO_4 (37.5% of AEC) in aqueous H_2O_2 -dioxane.

Besides the observation of the polyperoxo precursors, $^1\text{O}_2$ can also be directly observed with IRL (infrared luminescence). The near infrared detection of $^1\text{O}_2$ is based on the weak, spin forbidden relaxation of the excited, singlet molecular oxygen [$^1\text{O}_2$, $^1\Delta_g$] to its ground state, triplet molecular oxygen [$^3\text{O}_2$, $^3\Sigma_g^-$] (27, 28). Figure 3 shows this emission around 1276 nm for a LDH-Mo catalyst in a dioxane- H_2O_2 solution.

Catalyst Heterogeneity

In order to verify the true heterogeneity of the catalyst, an experiment was performed in which the catalyst was repeatedly filtered off from a hydrogen peroxide containing suspension and later resuspended into the solution (Fig. 4). After catalyst removal no further hydrogen peroxide conversion was monitored in time. Further evidence for catalyst heterogeneity was obtained in an attempt to measure the ^{95}Mo liquid NMR spectra for the molybdate or peroxomolybdate species of the catalyst in contact with hydrogen peroxide. No Mo signal was detected from the suspension or the clear supernatant even after extensive accumulations. This suggests that Mo is confined to the support and therefore not measurable in a liquid NMR experiment. Finally, elemental analyses of reaction solutions showed that molybdate concentrations in the reaction liquor were

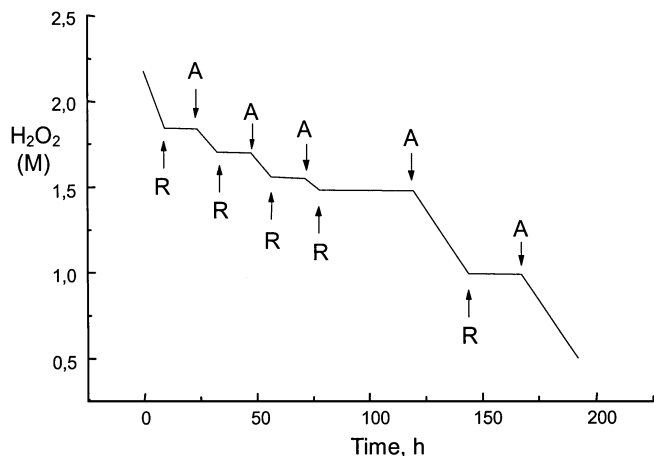


FIG. 4. Heterogeneity test in the LDH-Mo catalyzed H_2O_2 decomposition (H_2O_2 molarity as a function of time). The catalyst was repeatedly removed from the reaction suspension by centrifugation and filtration (R) and subsequently added again to the reaction filtrate (A). Reaction conditions: 200 ml methanol, 450 mmol H_2O_2 (35 wt% in H_2O), 30 mmol α -terpinene, 0.3 mmol MoO_4^{2-} on $\text{Mg}_{0.7}\text{Al}_{0.3}$ -LDH (AEC = 0.375), RT.

below the ICP detection limit (10 ppb), proving that less than 0.05% of the total Mo comes to the solution.

Basic Properties of the Layered Double Hydroxides

The literature shows that the catalytic properties of homogeneous molybdate are largely dependent not only on the hydrogen peroxide concentration, but also on the pH. In this study the basic properties of the LDHs were analyzed via three approaches: (i) *in vacuo* dried samples were mixed with a dye solution in toluene, followed by a benzoic acid titration (19, 20); (ii) alizarin, which is a pH sensitive dye, was adsorbed on samples dried *in vacuo*, and its diffuse reflectance spectrum was measured; (iii) XPS was used to determine the binding energy of the O 1s electrons;

prior to these XPS analyses, samples were calcined in order to avoid interference from nitrate–oxygen atoms (34, 35). Such a combined approach overcomes the limitations associated with each of the methods as such. Results are summarized in Table 3.

Acid titration of the basic sites in the presence of a pH indicator, such as bromothymol blue or phenolphthalein, provides a first indication of increasing total basicity upon decreasing aluminum content in Mg,Al-LDHs. Due to stacking of the layered double hydroxides in toluene, it is likely that only the external surfaces are titrated. Both the number of weaker basic sites (as measured in the titration with bromothymol blue) and the number of the stronger base sites (measured with phenolphthalein as indicator) increase steadily from $\text{Mg}_{0.7}\text{Al}_{0.3}$ -LDH to $\text{Mg}_{0.9}\text{Al}_{0.1}$ -LDH.

Measurement of the reflectance spectrum of LDH-adsorbed alizarin (1,2-dihydroxyanthraquinone) confirms this trend. Alizarin is red at pH 10.1 and turns to violet at pH 12.1. The maximum absorption shifts bathochromically with decreasing Al content, indicating a more pronounced basicity at lower aluminum content. However, these measurements may be influenced by electrostatic interactions between the conjugated system of the dye and the charged support.

Therefore, a supplementary analysis was performed by measuring the XPS O 1s binding energy, which is directly related to the basic strength of the oxygen atoms. A decreasing O 1s binding energy is related to increasing electron pair donation. As expected, the XPS analyses display the lowest binding energy for the sample with the lowest aluminum content. Finally, in order to probe the basic properties of the LDHs also in fully hydrated conditions, the pH values of aqueous suspensions containing equal amounts of LDH were measured. The pH increases from 9.1 for $\text{Mg}_{0.7}\text{Al}_{0.3}$ to 10.5 for $\text{Mg}_{0.9}\text{Al}_{0.1}$ -LDH. Based on all these indications, the supports with the highest Mg content clearly provide

TABLE 3
Characterization of Basic Properties of the LDH Supports

LDH nominal composition	pH of suspension in H_2O^a	mol basic sites per g LDH ^b		DRS ^c Alizarin (nm)	XPS ^d BE (eV)
		Bromothymol Blue ($\text{p}K_a = 7.1$)	Phenolphthalein ($\text{p}K_a = 9.3$)		
$\text{Mg}_{0.7}\text{Al}_{0.3}$ -LDH	9.1	1.33×10^{-4}	0.73×10^{-4}	518	531.4
$\text{Mg}_{0.8}\text{Al}_{0.2}$ -LDH	9.7	1.80×10^{-4}	1.03×10^{-4}	539	531.2
$\text{Mg}_{0.9}\text{Al}_{0.1}$ -LDH	10.5	2.74×10^{-4}	1.83×10^{-4}	549	531.1

^a Suspension of 1.5 g LDH in 100 ml deionized H_2O .

^b 0.15 g vacuum dried LDH, suspended in 2 ml indicator solution (0.1 mg/ml), is titrated with 0.01 M benzoic acid.

^c Wavelength of maximum absorption in diffuse reflectance spectroscopy: 0.15 g of vacuum dried LDH is mixed with 2 ml alizarin in toluene solution (0.1 mg/ml). Prior to analyses, samples are vacuum dried.

^d XPS analyses of calcined samples (calcination at 850°C).

the most basic environment to the molybdate anions and this may be reflected in the catalytic properties.

Catalytic Reactions: Effects of Catalyst Composition and Reaction Conditions

In this section, various factors that influence the singlet oxygenation with the molybdate LDH catalysts are investigated. Important output variables are (i) product selectivity and (ii) product yield, which at full conversion of H_2O_2 essentially reflects the efficiency of the oxidant use. Product selectivity is of particular interest, in order to discriminate between epoxidation, $^1\text{O}_2$ oxygenation, and radical-induced oxidations. In the latter context, the use of 1-methyl-1-cyclohexene as a diagnostic substrate allows a good discrimination between hydroperoxides formed via $^1\text{O}_2$ or via radicals (36, 37). These enyl hydroperoxides are reduced with PPh_3 after full consumption of the hydrogen peroxide, and the GC analysis of the allylic alcohols 1 to 3 in Table 4 results in characteristic distribution patterns. Particularly the fraction of allylic alcohol 2 is important: it is formed with at least 50% selectivity in a photosensitized reaction (e.g., with bengal rose, Table 4, entry 1), but is almost absent in a free radical reaction (Table 4, entry 2). The discrimination between epoxidation and $^1\text{O}_2$ oxygenation can be conveniently studied with either 2,3-dimethyl-2-butene or 1-methyl-1-cyclohexene.

For a good understanding of the results with the heterogeneous catalyst, it should be noted that for homogeneous MoO_4^{2-} catalysis, there are optimum values of pH

and $\text{H}_2\text{O}_2/\text{Mo}$ ratio, at which the rate of $^1\text{O}_2$ generation and the yield of $^1\text{O}_2$ products are maximal (29, 30, 38). If the pH is too high (e.g., 12.5), H_2O_2 may disproportionate spontaneously, or the peroxomolybdates are hydrolyzed by excess OH^- . In a too large excess of H_2O_2 , tetraperoxomolybdate $\text{MoO}(\text{O}_2)_4^{2-}$ is formed, and this complex only slowly releases $^1\text{O}_2$ (Scheme 1). The best results for $^1\text{O}_2$ oxygenation are generally obtained at a pH of about 10 and with a sufficient $\text{H}_2\text{O}_2/\text{Mo}$ ratio to promote the formation of the triperoxomolybdate $\text{MoO}(\text{O}_2)_3^{2-}$, which is the most labile $^1\text{O}_2$ precursor. When either the $\text{H}_2\text{O}_2/\text{Mo}$ ratio or the pH are lowered, epoxidation gradually predominates over $^1\text{O}_2$ formation. In such conditions, the average number of peroxo groups per Mo is lower than three. In literature, this epoxidation has been ascribed to the tetraperoxodimolybdate $\text{Mo}_2\text{O}_3(\text{O}_2)_4^{2-}$, which is in equilibrium with the diperoxomolybdate $\text{MoO}_2(\text{O}_2)_2^{2-}$ (39). A similar preference for epoxidation is expected for other species with a low number of peroxide groups per Mo; for instance, the monoperoxomolybdate $\text{MoO}_3(\text{O}_2)^{2-}$ cannot release $^1\text{O}_2$, but may well effect epoxidation (Scheme 1).

1. Molybdate loading of the catalyst. Table 4 shows results for different Mo concentrations on a fixed amount of LDH. The product distributions for the oxygenation of 1-methyl-1-cyclohexene are in agreement with oxygenation by $^1\text{O}_2$ (entries 3–5); radical oxidation or epoxidation are negligible. At first sight, it may seem of interest to have as many *active* sites as possible, in order to speed up the reaction. However, Table 4 indicates that the highest

TABLE 4
Oxidation of 1-Methyl-1-Cyclohexene with H_2O_2 and LDH-Mo: Effect of Molybdate Loading and Hydrophobicity/Hydrophilicity of the Catalyst

Entry	Product yields (%) ^a				
					
1. Sensitization (Bengal Rose) ^b	—	—	<i>31</i>	<i>50</i>	<i>19</i>
2. Radical oxidation ($\text{Fe}^{2+}/\text{H}_2\text{O}_2$) ^c	—	—	<i>39</i>	<i>7</i>	<i>54</i>
3. 37.5% AEC (28 $\mu\text{mol MoO}_4$)	0.6	5.2	11.6	2.3	
4. 25.0% AEC (18 $\mu\text{mol MoO}_4$)	0.6	5.8	12.2	2.9	
5. 12.5% AEC (10 $\mu\text{mol MoO}_4$)	0.9	8.9	19.1	6.4	
6. 12.5% AEC MoO_4 , 87.5% AEC pTOS	4.4	10.3	22.0	5.7	
7. 25.0% AEC MoO_4 , 75.0% AEC pTOS	4.9	9.3	21.5	3.9	

Note. Reaction conditions: 2.5 mmol 1-methyl-1-cyclohexene, 2 aliquots of 2.5 mmol H_2O_2 (35% in H_2O), 0.05 g $\text{Mg}_{0.7}\text{Al}_{0.3}$ -LDH in 3 ml 1,4-dioxane, 20°C.

^aProduct yields on substrate basis. AA, allylic alcohol. At complete H_2O_2 consumption, samples were taken and reduced with PPh_3 , then analyzed with GC.

^bReference reaction: $^1\text{O}_2$ oxygenation.

^cReference reaction: free radical oxidation ($\text{FeSO}_4 \cdot 7\text{H}_2\text{O} + \text{H}_2\text{O}_2$). Italic numbers in entries 1 and 2 give the relative ratios of the allylic alcohols.

seems that with $\text{Mg}_{0.9}\text{Al}_{0.1}$ -LDH, which is the most basic support, the formation of such species is sufficiently suppressed to avoid significant epoxidation.

It was not attempted to use a support with an even lower aluminum content than 10% of the octahedral ions. First, more and more brucite will be present in the materials at higher Mg concentration, and second, the decrease of the Al content also lowers the anion exchange capacity of the LDH, which may ultimately lead to bad retention of the molybdate on the catalyst.

Catalyst stability and heterogeneity were confirmed for a $\text{Mg}_{0.9}\text{Al}_{0.1}$ -Mo catalyst in a recycling experiment. Both the fresh catalyst and the recycled catalyst yield similar oxygenation yields (Table 5).

4. Temperature. In addition to molybdate loading, basicity, and hydrophilicity/hydrophobicity of the catalyst, temperature provides another parameter to control the chemical reaction rate. Figure 5 presents for reactions at different temperatures the final $^1\text{O}_2$ -oxygenate yields from 1-methyl-1-cyclohexene and 2,3-dimethyl-2-butene, upon complete consumption of H_2O_2 .

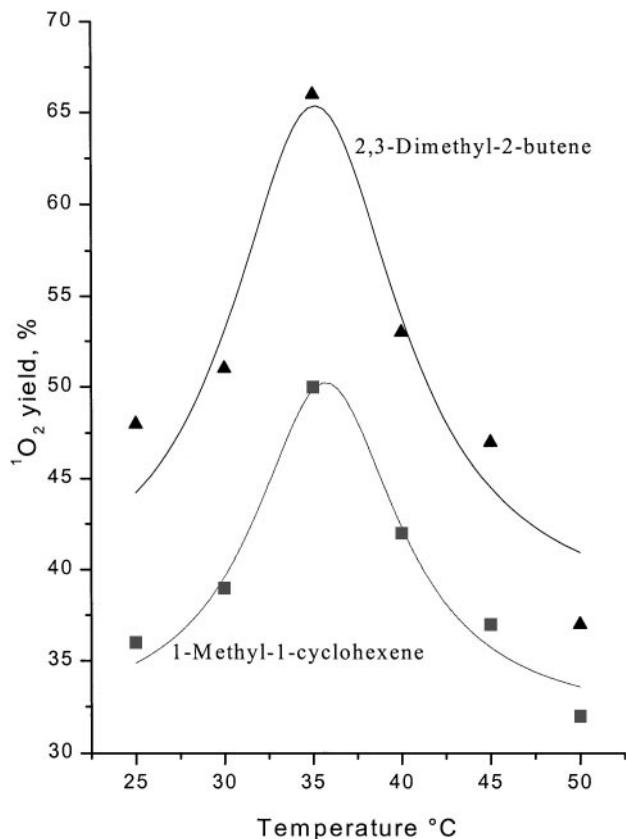


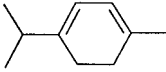
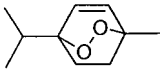
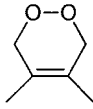
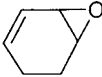
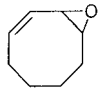
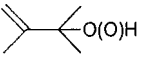
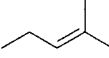
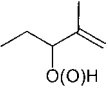
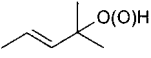
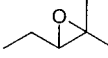
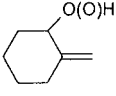
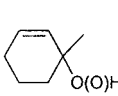
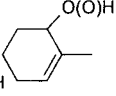
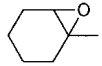
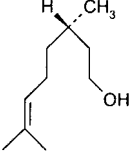
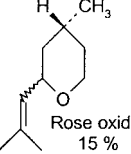
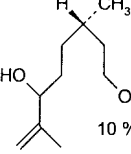
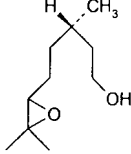
FIG. 5. Temperature effect on the oxidation of 1-methyl-1-cyclohexene or 2,3-dimethyl-2-butene. Yields of hydroperoxides, reduced to allylic alcohols ($^1\text{O}_2$ yield) at complete consumption of H_2O_2 are plotted vs reaction temperature. Conditions: 2.5 mmol olefin, H_2O_2 (5 mmol, added in two portions), 0.05 g $\text{Mg}_{0.9}\text{Al}_{0.1}$ -LDH- MoO_4 (10 $\mu\text{mol MoO}_4^{2-}$); 3 ml 1,4-dioxane.

A clear reaction optimum is observed around 35°C . The decreasing yield of $^1\text{O}_2$ oxygenates with increasing reaction temperature from 35°C upward can be caused by several elements. First, the $^1\text{O}_2$ lifetime decreases with increasing environment temperature (40). Second, a too fast hydrogen peroxide conversion into $^1\text{O}_2$ is likely to result in self-annihilation of $^1\text{O}_2$ (Scheme 2, B), or in an oxygenation that is limited by the depletion of the substrate around the catalyst particles. Use of hydrogen peroxide at more elevated temperatures may entail risks of creating free radicals, particularly if traces of metals are mixed with peroxide solutions. However, the allylic alcohol distribution obtained in the reaction of 1-methyl-1-cyclohexene at 50°C is still in full agreement with that of a true $^1\text{O}_2$ reaction. At this point, the reason for the decreasing oxygenate yields at temperatures lower than 35°C is unclear. Anyway, in order to have optimum rate and oxygenate yield, a reaction temperature of 35°C seems most appropriate.

Table 6 shows $^1\text{O}_2$ oxidation reactions for some different substrates. In these reactions, oxygenate yield and selectivity for the $^1\text{O}_2$ products are optimized via choice of appropriate reaction conditions, namely 35°C , and a hydrophilic LDH support with a sufficiently alkaline character ($\text{Mg}_{0.9}\text{Al}_{0.1}$) and with low Mo content (0.2 mmol per g). Since only two equivalents of H_2O_2 were used per equivalent of organic substrate, a 100% yield can be obtained only if there is no physical quenching whatsoever of $^1\text{O}_2$ by the solvent, the substrate, or the support. Efficient endoperoxidations ($[4\pi + 2\pi]$ -cycloadditions) are observed for 1,3-dienes, with yields up to 77%. Higher yields are achieved for more electron-rich substrates such as α -terpinene in comparison with the unsubstituted 1,3-cyclohexadiene. Molecules with an extended ring are known to be less susceptible to $^1\text{O}_2$, which explains the decreased reaction yield for 1,3-cyclooctadiene (1). The trends observed in the "ene reactions" are similar to those observed in the endoperoxidations: higher peroxidation yields are obtained for the more electron-rich alkenes such as 2,3-dimethyl-2-butene than for the more electron-poor β -citronellol. Thus it seems that the susceptibility of the molecules to $^1\text{O}_2$ in these heterogeneously catalyzed reactions parallels their reactivity in homogeneous conditions; there is no clear evidence for an effect of the support on the reaction at 35°C between the organic substrate and $^1\text{O}_2$.

5. Solvent effects. Table 7 shows rates for disproportionation of hydrogen peroxide by LDH- MoO_4 in different solvents. Unlike the substrate oxygenation, these disproportionation rates cannot be affected by solvent quenching of $^1\text{O}_2$ and thus directly reflect the solvent effects on the activity of the heterogeneous Mo catalyst. The observed solvent effects may originate in the formation of the peroxomolybdate species, or in the subsequent disproportionation of these species into $^1\text{O}_2$; even differences between the dispersibility of the catalyst in the various solvents may be

TABLE 6
Oxygenation of Various Substrates with $^1\text{O}_2$ Generated by the LDH-Mo/ H_2O_2 System at 35°C

Substrate	$^1\text{O}_2$ yield	Epoxide yield
 α -Terpinene	 77%	<1%
 2,3-Dimethyl-1,3-butadiene	 62%	 5%
 1,3-Cyclohexadiene	 61%	 1%
 <i>cis</i> , <i>cis</i> -1,3-Cyclooctadiene	 54%	 4%
 2,3-Dimethyl-2-butene	 66%	 4%
 2-Methyl-2-pentene	 25%  37% 62%	 1%
 1-Methyl-1-cyclohexene	 18%  24%  7% 50%	 <1%
 (-)- β -Citronellol	 Rose oxide 15%  10% rose oil ^a 25%	 1%

Note. Reaction conditions: 1.25 mmol substrate, 2 aliquots of 1.25 mmol H_2O_2 (35% in H_2O), 1.5 ml 1,4-dioxane, 0.025 g $\text{Mg}_{0.9}\text{Al}_{0.1}\text{-MoO}_4$ ($5 \mu\text{mol MoO}_4^{2-}$), 35°C. Sampling after full hydrogen peroxide conversion, about 8 h.

^a Obtained after PPh_3 reduction and acidification of the sample with HCl.

important. The rate is highest in water, but this solvent is as such obviously unsuitable for oxygenation of organic compounds. Of the four other, H_2O_2 miscible organic solvents in Table 7, the rate is lowest for the reaction in methanol.

Table 8 describes a series of eight solvents, the yields and selectivities of the reactions with 1-methyl-1-cyclohexene.

These reactions were performed at 35°C, with a catalyst with a relatively small Mo concentration and a high Mg content. For all reactions, the hydroperoxide (or allylic alcohol) distribution patterns are in satisfactory agreement with $^1\text{O}_2$ oxygenation. While the hydroperoxide selectivity is generally excellent, small but significant increases in epoxide

TABLE 7

Rate Constant for Hydrogen Peroxide Decomposition on a LDH-Mo Catalyst in Different Solvents

Solvent	Rate, M (mol Mo) ⁻¹ s ⁻¹
Acetone	0.323
1,4-Dioxane	0.312
Ethanol	0.46
Methanol	0.241
Water	1.071

Note. Reaction conditions: 0.2 g Mg_{0.7}Al_{0.3}-LDH-Mo (MoO₄²⁻: 37.5% of AEC), 50 mmol H₂O₂ (35% in H₂O), 25 ml solvent, RT.

selectivity are observed for methanol and acetonitrile. In the case of acetonitrile, base-catalyzed epoxidation may occur via formation of a peroxyimide acid from acetonitrile and H₂O₂ (41, 42); however, the coproduct of such an oxidation, acetamide, was not detected in the reaction mixture, which rules out that solvent oxidation is playing a role. In the case of methanol, competition between the solvent and H₂O₂ for coordination on the molybdate is a likely reason for the increased epoxide formation (2). Even if the red color of the suspension of the catalyst in methanol qualitatively indicates that even tetraperoxomolybdate species are formed, the competing effect of methanol might increase the fraction of lower peroxomolybdate species, which are capable of epoxidation. A slight inhibitory effect of MeOH in the formation of the peroxomolybdates also successfully accounts for the lower reaction rates in methanol (Table 7).

It was attempted to relate the variations of the allylic alcohol yields in Table 8 to properties of the solvent. Comparison with the known lifetimes (τ_{Δ}) of ¹O₂ in all these sol-

vents does not reveal a clear correlation (1, 43). At least this proves that with our optimized catalyst (e.g., low Mo content, high Mg content) and conditions (e.g., sufficient substrate concentration), major deactivation of ¹O₂ by the solvent is avoided. A better correlation is obtained with the π^* solvent parameter, the so-called “dipolarity–polarizability” parameter. For instance, the highest hydroperoxide yields are obtained in acetonitrile and DMF, which happen also to have the highest π^* values of the solvents in Table 8. This correlation may be rationalized in various ways. First, it has been proposed that solvents with a high π^* value can better stabilize the ¹[substrate-O₂] exciplex, which probably has some charge transfer character, and from which the oxygenated products are eventually formed (43, 44). In an alternative hypothesis, an increasing solvent dipolarity may improve the dispersibility of the hydrophilic catalyst in the organic medium; in such a case, a positive effect of the solvent polarity on the oxygenate yield is expected as well. Further subtle differences between the solvents may be ascribed to a combination of π^* and ¹O₂ lifetime effects; for instance, in the comparison between acetonitrile and DMF, the lower lifetime in DMF is compensated by its higher π^* value, and eventually about the same oxygenate yields are obtained. Overall, in view of the high hydroperoxide yield and selectivity, and because its relatively low boiling point facilitates workup, 1,4-dioxane is an excellent choice.

CONCLUSIONS

Molybdate exchanged LDHs are excellent and truly heterogeneous catalysts for conversion of H₂O₂ into ¹O₂. For various Mo contents of the catalyst, and for different Mg/Al ratios in the octahedral layer, Mo is predominantly present as monomeric molybdate. In contact with H₂O₂, singlet

TABLE 8

Solvent Effects on the Oxidation of 1-Methyl-1-Cyclohexene by the LDH-Mo Catalyst, and Comparison with the ¹O₂ Lifetime (τ_{Δ}) and the Solvent π^* Parameter

Solvent	τ_{Δ} (μ s) ^a	π^* ^a	Yield AA, ^b %	Yield epoxide, ^b %	AA 1 ^b %	AA 2 ^b %	AA 3 ^b %
Acetonitrile	62	0.75	68	0.6	36	47	17
DMF	12	0.88	66	0.2	39	46	15
Acetone	50	0.71	55	0.2	38	47	16
Dioxane	30	0.55	50	0.2	37	48	15
Methanol	9.5	0.60	50	0.8	33	48	18
THF	22	0.58	44	0.2	39	46	15
Ethanol	12	0.54	40	0.5	36	47	17
2-propanol	22.1	0.48	40	0.4	34	49	16

Note. Reaction conditions: 1.25 mmol 1-methyl-1-cyclohexene, 2 aliquots of 1.25 mol H₂O₂ (35% in H₂O), 1.5 ml solvent, 0.025 g Mg_{0.9}Al_{0.1}-MoO₄ (5 μ mol MoO₄²⁻), 35°C. Sampling after complete hydrogen peroxide conversion. Samples reduced with PPh₃.

^a τ_{Δ} , ¹O₂ lifetime; π^* , solvent dipolarity–polarizability parameter, Ref. 23.

^b Yields are given on substrate basis. AA, allylic alcohol; see Table 4. The distribution over AA1, AA2 and AA3 is given in% of the total amount AA.

oxygen is formed at the surface, as is evidenced for instance by the NIR luminescence spectra. Next, $^1\text{O}_2$ diffuses away from the $^1\text{O}_2$ generating centers, in order to react with dienes or alkenes. A high dipolarity/polarizability of the solvent has a clearly positive effect on these oxygenations. In order to maximize the efficiency of H_2O_2 use, and in order to minimize the epoxidation, it is advisable to limit the Mo content of the catalyst, to use a hydrophilic molybdate-exchanged LDH, and to work with LDHs with a high Mg content in the octahedral layer. As was proved by various procedures to study the surface basicity, the latter provide a more basic microenvironment to the catalytic molybdate anions.

REFERENCES

- Frimer, A. A., "Singlet Oxygen." Vols. I-IV. CRC Press, Boca Raton, FL, 1985.
- Sheldon, R. A., and Kochi, J. K., "Metal-Catalyzed Oxidations of Organic Compounds." Academic Press, San Diego, 1981.
- Midden, R. A., and Wang, S. Y., *J. Am. Chem. Soc.* **105**, 4129 (1983).
- Blossey, E. C., Neckers, D. C., Thayer, A. L., and Schaap, A. P., *J. Am. Chem. Soc.* **95**, 5820 (1973).
- Schaap, A. P., Thayer, A. L., Blossey, E. C., and Neckers, D. C., *J. Am. Chem. Soc.* **97**, 3741 (1975).
- Neckers, D. C., Blossey, E. C., and Schaap, A. P., U.S. patent 4315998 (1982).
- Nowakowska, M., Sustar, E., and Guillet, J. E., *Photochem. Photobiol. A* **80**, 369 (1994).
- Quast, H., Dietz, T., and Witzel, A., *Liebigs Ann.* 1495 (1995).
- DiMagno, S. G., Dussault, P. H., and Schultz, J. A., *J. Am. Chem. Soc.* **118**, 5312 (1996).
- Gekhman, A. E., Moiseeva, N. I., and Moiseev, I. I., *Russ. Chem. Bull.* **44**, 584 (1995).
- Bacon, R. G. R., and Kuan, L. C., *Tetrahedron Lett.* 3397 (1971).
- Hayashi, Y., Shioi, S., Togami, M., and Sakan, T., *Chem. Lett.* 651 (1973).
- Aubry, J. M., *J. Am. Chem. Soc.* **107**, 5844 (1985).
- Aubry, J. M., and Bouttemy, S., *J. Am. Chem. Soc.* **119**, 5286 (1997).
- McGoran, E. C., and Wyborney, M., *Tetrahedron Lett.* **30**, 783 (1989).
- van Laar, F., De Vos, D., Vanoppen, D., Sels, B., Jacobs, P. A., Del Guerzo, A., Pierard, F., and Kirsch-De Mesmaeker, A., *Chem. Commun.* 267 (1998).
- Cavani, F., Trifirò, F., and Vaccari, A., *Catal. Today* **11**, 173 (1991).
- Drezdzon, M. A., U.S. patent 4774212 (1988).
- Tanabe, K., Misono, M., Ono, Y., and Hattori, H., *Stud. Surf. Sci. Catal.* **51**, (1989).
- Tanabe, K., "Solid Acids and Bases, Their Catalytic Properties." Kodansha International, Tokyo, 1970.
- Ando, W., "Organic Peroxides." Wiley, New York, 1992.
- Miyata, S., *Clays Clay Miner.* **28**, 50 (1980).
- Drezdzon, M. A., *Inorg. Chem.* **27**, 4628 (1988).
- Wagner, C. D., Riggs, W. M., Davis, L. E., Moulder, J. F., and Muilenberg, G. E., "Handbook of X-ray Photoelectron Spectroscopy." Perkin Elmer, Palo Alto, CA, 1979.
- Gardner, E., and Pinnavaia, T. J., *Appl. Catal. A* **67**, 65 (1998).
- Niemantsverdriet, J. W., "Spectroscopy in Catalysis." VCH, 1995.
- Foote, C. S., and Niu, Q. J., *Inorg. Chem.* **31**, 3472 (1992).
- Böhme, K., and Brauer, H. D., *Inorg. Chem.*, **31**, 3468 (1992).
- Nardello, V., Marko, J., Vermeersch, G., and Aubry, J. M., *Inorg. Chem.* **34**, 4950 (1995).
- Nardello, V., Bouttemy, S., and Aubry, J. M., *J. Mol. Cat. A* **117**, 439 (1997).
- Csányi, L. J., Horváth, I., and Galbács, Z. M., *Transition Met. Chem.* **14**, 90 (1989).
- Csányi, L. J., *Transition Met. Chem.* **14**, 298 (1989).
- Csányi, L. J., *Transition Met. Chem.* **15**, 371 (1990).
- Okamoto, Y., Ogawa, M., Maezawa, A., and Imanaka, T., *J. Catal.* **112**, 427 (1988).
- Hattori, H., *Chem. Rev.* **95**, 537 (1995).
- van Laar, F. M. P. R., De Vos, D. E., Vanoppen, D. L., Pierard, F., Brodtkorb, A., Kirsch-De Mesmaeker, A., and Jacobs, P. A., in "Proceedings, 12th International Zeolite Conference (M. M. J. Treacy, B. K. Marcus, M. E. Bisher, and J. B. Higgins, Eds.) MRS (1999) 1213.
- Pettit, T. L., and Fox, M. A., *J. Phys. Chem.* **90**, 1353 (1986).
- Aubry, J. M., and Cazin, B., *Inorg. Chem.* **27**, 2013 (1988).
- Campbell, N. J., Dengel, A. C., Edwards, C. J., and Griffith, W. P., *J. Chem. Soc. Dalton Trans.* 1203 (1989).
- Schmidt, R., and Brauer, H.-D., *J. Am. Chem. Soc.* **109**, 6976 (1987).
- Payne, G. B., *Tetrahedron* **18**, 763 (1962).
- Ueno, S., Yamaguchi, K., Yoshida, K., Ebitani, K., and Kaneda, K., *Chem. Commun.* 295 (1998).
- Aubry, J. M., Mandard-Cazin, B., Rougee, M., and Bensasson, R. V., *J. Am. Chem. Soc.* **117**, 9159 (1995).
- Clennan, E. L., *Tetrahedron* **47**, 1343 (1991).